

Single Axis Pointing for Underactuated Spacecraft with a Residual Angular Momentum

By Alessandro ZAVOLI,¹⁾ Fabrizio GIULIETTI,²⁾ Giulio AVANZINI,³⁾ Guido DE MATTEIS,¹⁾

¹⁾*Department of Mechanical and Aerospace Engineering, 'Sapienza' Università di Roma, Rome, Italy*

²⁾*Department of Industrial Engineering, Università di Bologna (Forlì Campus), Forlì, Italy*

³⁾*Department of Engineering for Innovation, Università del Salento, Lecce, Italy*

(Received April 17st, 2017)

The problem of aiming a body-fixed axis along an inertially fixed direction is dealt with, when only two reaction wheels can exchange angular momentum with the spacecraft platform. The feasibility of the pointing maneuver for an arbitrary body-fixed axis is assessed in the presence of a non-zero angular momentum for the system. Two control laws are then developed, which allow for completing the desired pointing maneuver from arbitrary initial conditions. Performance two controllers are compared by means of numerical simulation for a configuration representative of a small-size satellite.

Key Words: Spacecraft attitude control, Attitude dynamics, Underactuated system, Reaction wheel failure

1. Introduction

The present paper explores the feasibility of single-axis pointing maneuvers for an underactuated spacecraft in the presence of a non-zero residual angular momentum vector. In the considered operational scenario, a body-fixed axis $\hat{\sigma}$, such as the line-of-sight of a sensor, a nozzle for orbit control or an antenna, needs to be aligned to a target direction $\hat{\tau}$, fixed in the inertial reference frame. Only two reaction wheels are available, a situation representative of a failure condition in non-redundant control systems or of a critical condition after multiple failures of a reaction wheel cluster. Two control laws are proposed to attain the prescribed pointing starting from arbitrary initial conditions, employing only two reaction wheels.

Recent advances in spacecraft and satellite control systems have succeeded in solving several challenging problems concerning attitude tracking, robust control, optimal slew maneuvers, or precision pointing, while assuming a number of actuators equal to, or larger than, the degrees of freedom of the system. In the attempt of extending operational lifetime or increasing mission resilience to system failures, attitude stabilization problems in case of actuator failures is being gaining an increasing attention.

A review of attitude control problems for underactuated spacecraft is presented by Tsiotras.¹⁾ Several authors dealt with these problems, considering diverse types of control hardware (thruster,²⁾ reaction wheels,³⁾ control momentum gyro⁴⁾), for either axis-symmetric⁵⁾ or tri-inertial⁶⁾ spacecraft, in different mission scenarios, such as full attitude stabilization, single-axis pointing, acquisition of a desired spin state, etc.

The present paper aims at extending the results derived in Zavoli et al.,⁷⁾ where a single-axis pointing maneuver for a tri-inertial spacecraft is studied under the hypothesis of zero total angular momentum, to the case where an arbitrary, non-zero, initial angular momentum is present. The feasibility of the pointing maneuver is analytically determined for a generic body-fixed axis $\hat{\sigma}$, highlighting that, when $\hat{\sigma}$ is not a principal axis of inertia, it cannot be aligned along some inertial directions $\hat{\tau}$,

while keeping the spacecraft at rest. In this respect, the present work also extends the results proposed by Yoon⁸⁾ and Kwon,⁹⁾ where a similar problem was considered, but the analysis was restricted to the circumstance where a principal axis of inertia was to be pointed.

When the pointing maneuver is feasible, a command law for the two active reaction wheels is sought, which asymptotically drives the body-fixed direction $\hat{\sigma}$ towards $\hat{\tau}$, so that the pointing error, that is, the angle between the unit vectors $\hat{\sigma}$ and $\hat{\tau}$, asymptotically approaches zero.

In the next section, after a short review of spacecraft dynamics in underactuated conditions, the attitude profile allowing for the desired alignment is derived, together with a simple analytical condition for maneuver feasibility. Spacecraft attitude is represented in terms of precession, nutation, and spin angles, that provide a clear and intuitive physical interpretation of the results (i.e. the final value of the spin angle indicates the distribution of angular momentum between the wheels, when the spacecraft is at rest). Also, this attitude representation allows for the definition of two control strategies, presented in Sections 3. and 4., which asymptotically drive the spacecraft towards the prescribed alignment.

The first command law, discussed in Section 3., will be referred to as Controller A. It is based on a two-step strategy, where the first step reduces the residual angular speed below a prescribed threshold, while driving the spin angle close to the prescribed value. The reduction of the angular rate close to zero also drives the nutation angle towards its final value, equal to $\pi/2$ for all admissible pointing conditions. The second step, performed under the action of a Linear Quadratic Regulator, drives the precession angle towards the required value for accurate pointing, stabilizing the spacecraft in the neighborhood of the desired final attitude, achieving the prescribed pointing with zero residual angular rate. In this case a formal proof of convergence to the desired final state is available for both controllers.

In Section 4., a second control law is developed, referred to as Controller B, based on the definition of a desired angular velocity command, which enforces a stable first order dynamics

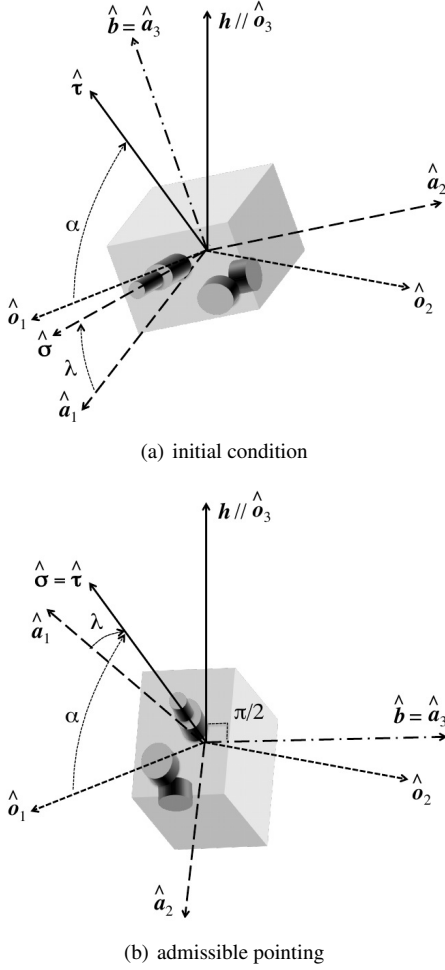


Figure 1. Geometry of the problem

to the precession angle towards its desired final value. The nonlinear equations of motion for spacecraft attitude dynamics are recast in error form, highlighting the angular velocity tracking error, as well as the spacecraft attitude error with respect to the target attitude. A nominal dynamics is isolated from a vanishing perturbation term. A rigorous proof of stability is derived for the stability of the nominal part of the system, only. Robustness of the stability of the nominal system with respect to the vanishing perturbation is then investigated by means of numerical simulations in Section 5., where performance of both control laws are compared and discussed. A section of concluding remarks ends the paper.

2. Problem Statement and Mathematical Model

2.1. Spacecraft Dynamics

A satellite platform equipped with three identical reaction wheels is considered. The spin axes of the wheels are assumed aligned with the principal axes of inertia of the rigid body.

An underactuation condition is considered, that is, a (failed) wheel cannot provide torque. Let $\mathcal{F}_B = \{G; \hat{e}_1, \hat{e}_2, \hat{e}_3\}$ be a body-fixed reference frame, centered in the spacecraft center of mass, G , with axes aligned to the principal axes of inertia of the spacecraft. Without loss of generality, the spin axis of the failed wheel, \hat{b} is assumed to be aligned to the third axis of the body frame, that is, $\hat{b} \equiv \hat{e}_3$. As a consequence, only two reaction

wheels are available for control, with spin axes parallel to the \hat{e}_1 and \hat{e}_2 body axes, respectively.

Hereafter, it is also assumed that no external torque is present, so that the angular momentum vector is constant in the inertial frame. As a further hypothesis, the magnitude of the angular momentum is also assumed that to be of magnitude less than the momentum storage capacity of the single active wheel. This is a mild assumption, provided that, if this condition is violated, it would not be possible to attain any fixed attitude. In this respect, one can assume that a desaturation maneuver already reduced the overall angular momentum below an acceptable threshold for operating the spacecraft.

Under the above hypothesis, and expressing all vector quantities in terms of components in the body-fixed set of principal axes of inertia, spacecraft dynamics is given by

$$\dot{\mathbf{H}} + \boldsymbol{\omega}^\times \mathbf{H} = \mathbf{0} \quad (1)$$

where

$$\mathbf{H} = \mathbf{J}\boldsymbol{\omega} + \mathbf{h} \quad (2)$$

is the total angular momentum vector of the system, whose magnitude $H_0 = \|\mathbf{H}\|$ is constant, $\boldsymbol{\omega} = (\omega_1, \omega_2, \omega_3)^T$ is the angular velocity vector of the body frame with respect to the inertial frame, $\mathbf{J} = \text{diag}(J_1, J_2, J_3)$ is the inertia tensor (including the contribution of RW at rest), $\mathbf{h} = (h_1, h_2, 0)^T$ is the relative angular momentum of the reaction wheels, under the assumption of a failed wheel aligned with \hat{e}_3 , and

$$\mathbf{v}^\times = \begin{bmatrix} 0 & -v_3 & v_2 \\ v_3 & 0 & -v_1 \\ -v_2 & v_3 & 0 \end{bmatrix}$$

indicates the skew-symmetric matrix equivalent for the cross-product operation associated to the vector $\mathbf{v} = (v_1, v_2, v_3)^T$.

The relative angular momentum of the i -th reaction wheel is equal to $h_i = J_w \Omega_i$, where Ω_i is the wheel spin rate relative to \mathcal{F}_B , whereas the absolute angular momentum for the same wheel is given by $h_i^{(a)} = J_w(\Omega_i + \omega_i) = h_i + J_w \omega_i$. The dynamics of the i -th wheel, under the control of the electrical motor torque $g_{em,i}$, is thus given by

$$\dot{h}_i^{(a)} = \dot{h}_i + J_w \dot{\omega}_i = g_{em,i} \quad i = 1, 2 \quad (3)$$

A vector $\mathbf{u} = (u_1, u_2, 0)^T$ of virtual control torques, $u_i = -\dot{h}_i = -(g_{em,i} - J_w \dot{\omega}_i)$, is introduced to attain a more compact notation. As a result, the mathematical model of the spacecraft dynamics with two reaction wheels is

$$\dot{\boldsymbol{\omega}} = \mathbf{J}^{-1} [\mathbf{u} - \boldsymbol{\omega}^\times (\mathbf{J}\boldsymbol{\omega} + \mathbf{h})] \quad (4)$$

$$\dot{\mathbf{h}} = -\mathbf{u} \quad (5)$$

2.2. Kinematics

The single-axis pointing problem requires that the spacecraft achieves a final attitude, where a body-fixed axis, identified by the unit vector $\hat{\sigma}$, is aligned to a prescribed inertially-fixed direction $\hat{\tau}$, with zero final angular speed. Without loss of generality, an inertially fixed reference frame $\mathcal{F}_I = \{G; \hat{\delta}_1, \hat{\delta}_2, \hat{\delta}_3\}$ is introduced, such that the total angular momentum of the spacecraft \mathbf{H} is aligned with $\hat{\delta}_3$, and the axis $\hat{\tau}$ lies in the $\hat{\delta}_1$ - $\hat{\delta}_3$ plane, whereas $\hat{\delta}_2 = \hat{\delta}_3 \times \hat{\delta}_1$ completes a right-handed triad. One thus has

$$\hat{\delta}_1 = \hat{\delta}_2 \times \hat{\delta}_3; \quad \hat{\delta}_2 = (\mathbf{H} \times \hat{\tau}) / \|\mathbf{H} \times \hat{\tau}\|; \quad \hat{\delta}_3 = \mathbf{H} / \|\mathbf{H}\| \quad (6)$$

Note that the unit vector $\hat{\boldsymbol{d}}_1$ is parallel to the direction of the projection of $\hat{\boldsymbol{r}}$ on the plane perpendicular to \boldsymbol{H} . In the peculiar case when $\hat{\boldsymbol{r}}$ is parallel to \boldsymbol{H} , $\hat{\boldsymbol{d}}_1$ and $\hat{\boldsymbol{d}}_2$ can be selected arbitrarily on the plane perpendicular to $\hat{\boldsymbol{d}}_3$, to complete an orthogonal right-handed triad \mathcal{F}_I .

Spacecraft attitude with respect to \mathcal{F}_I can be represented by means of a 3-1-3 sequence of precession (Ψ), nutation (Θ), and spin (Φ) Euler angles,¹⁰ where $\Psi \in [-\pi, \pi]$, $\Theta \in [0, \pi]$, and $\Phi \in [-\pi, \pi]$. The coordinate transformation matrix between inertial and body frame is $\mathbb{T}_{BI} = \mathbb{R}_3(\Phi) \mathbb{R}_1(\Theta) \mathbb{R}_3(\Psi)$, where $\mathbb{R}_i(\alpha)$ for $i = 1, 3$ is the elementary rotation matrix,¹¹ which provides the coordinate transformation between two frames displaced by a rotation α around the i -th coordinate axis, and

$$\mathbb{T}_{BI} = \begin{bmatrix} c\Phi c\Psi - s\Phi c\Theta s\Psi & c\Phi s\Psi + s\Phi c\Theta c\Psi & s\Phi s\Theta \\ -s\Phi c\Psi - c\Phi c\Theta s\Psi & c\Phi c\Theta c\Psi - s\Phi s\Psi & c\Phi s\Theta \\ s\Theta s\Psi & -s\Theta c\Psi & c\Theta \end{bmatrix} \quad (7)$$

where $s\alpha = \sin \alpha$ and $c\alpha = \cos \alpha$.

The evolution of Euler angle rates as a function of angular speed is given by

$$\begin{pmatrix} \dot{\Psi} \\ \dot{\Theta} \\ \dot{\Phi} \end{pmatrix} = \begin{bmatrix} \sin \Phi / \sin \Theta & \cos \Phi \sin \Theta & 0 \\ \cos \Phi & -\sin \Phi & 0 \\ -\sin \Phi / \tan \Theta & -\cos \Phi / \tan \Theta & 1 \end{bmatrix} \begin{pmatrix} \omega_1 \\ \omega_2 \\ \omega_3 \end{pmatrix} \quad (8)$$

The attitude representation is known to be singular when $\Theta = 0, \pi$. Nonetheless, this attitude parametrization is particularly beneficial for the problem under investigation, as it simplifies the determination of the attitude which achieves the desired pointing, as outlined in the next subsection.

2.3. Feasibility and Solution of the Pointing Problem

When a spacecraft with only two active RW's is considered, the constraint of constant non-zero angular momentum restricts the set of admissible attitudes at rest to a compact subset of $\text{SO}(3)$, provided that the total angular momentum of the whole satellite must lie in the plane identified by the spin axes of the two active reaction wheels (plane $\hat{\boldsymbol{e}}_1$ - $\hat{\boldsymbol{e}}_2$, under the assumptions outlined above for the spacecraft model).

Given the definition of the body and inertial reference frames \mathcal{F}_B and \mathcal{F}_I , respectively, the target direction $\hat{\boldsymbol{r}}$ can be expressed in \mathcal{F}_I as

$$\hat{\boldsymbol{r}}_I = (\cos \alpha, 0, \sin \alpha)^T$$

where $\alpha \in [-\pi/2, \pi/2]$ is the elevation of $\hat{\boldsymbol{r}}$ over the $\hat{\boldsymbol{e}}_1$ - $\hat{\boldsymbol{e}}_2$ plane.

On the other hand, the unit vector $\hat{\boldsymbol{\sigma}}$ can be parametrized in \mathcal{F}_B as

$$\hat{\boldsymbol{\sigma}} = (\cos \lambda \cos \eta, \cos \lambda \sin \eta, \sin \lambda)^T \quad (9)$$

where λ is the elevation over the $\hat{\boldsymbol{e}}_1$ - $\hat{\boldsymbol{e}}_2$ plane and η is the azimuth with respect to $\hat{\boldsymbol{e}}_1$. Provided that the frame \mathcal{F}_B can always be chosen such that $\hat{\boldsymbol{e}}_3^T \hat{\boldsymbol{\sigma}} \geq 0$, the analysis can be restricted, without loss of generality, to the case $\lambda \in [0, \pi/2]$.

In order to simplify the derivation of the target attitude, an auxiliary body-fixed reference frame $\mathcal{F}_A = \{G; \hat{\boldsymbol{a}}_1, \hat{\boldsymbol{a}}_2, \hat{\boldsymbol{a}}_3\}$ is introduced, obtained rotating \mathcal{F}_B by an angle η about the axis $\hat{\boldsymbol{e}}_3$, that is, $\mathbb{T}_{AB} = \mathbb{R}_3(\eta)$. As a consequence, the auxiliary reference frame can be parametrized by means of a 3-1-3 set of Euler angles, $\{\Psi', \Theta', \Phi'\}$, such that $\Phi' = \Phi + \eta$, $\Theta' = \Theta$, and $\Psi' = \Psi$.

In this auxiliary reference frame, the unit vector $\hat{\boldsymbol{\sigma}}$ belongs to the plane $\hat{\boldsymbol{a}}_1$ - $\hat{\boldsymbol{a}}_3$, so that its components are given by

$$\hat{\boldsymbol{\sigma}}_A = (\cos \lambda, 0, \sin \lambda)^T \quad (10)$$

The derivation of the maneuver feasibility condition and the determination of the final admissible attitude which guarantees the prescribed alignment of $\hat{\boldsymbol{\sigma}}$ and $\hat{\boldsymbol{r}}$ with zero residual angular rate are performed describing spacecraft attitude with respect to this auxiliary reference frame

Starting from an arbitrary initial attitude, identified by the angles Ψ_i, Θ_i , and Φ_i , the final attitude represented by Ψ_f, Θ_f , and Φ_f must satisfy the following constraints

1. the spacecraft is at rest, that is, $\boldsymbol{\omega} = 0$;
2. $\hat{\boldsymbol{\sigma}}$ is aligned with $\hat{\boldsymbol{r}}$, that is, $\hat{\boldsymbol{\sigma}} = \hat{\boldsymbol{r}}$.

The first condition requires that, at the end of the maneuver, the total angular momentum is completely stored in the reaction wheels, that is, \boldsymbol{H} must lie on the $\hat{\boldsymbol{a}}_1$ - $\hat{\boldsymbol{a}}_2$ plane, which implies $\hat{\boldsymbol{a}}_3^T \boldsymbol{H} = 0$. Remembering that total angular momentum is parallel to $\hat{\boldsymbol{d}}_3$, so that $\boldsymbol{H}_I = (0, 0, H_0)^T$, and $\boldsymbol{H} = \mathbb{T}_{BI} \boldsymbol{H}_I$, this condition can be expressed as $h_3 = H_0 \cos \Theta = 0$.

Thus, the first requirement is met if $\cos \Theta_f = 0$, that is, the nutation angle at the end of the pointing maneuver is $\Theta_f = \pi/2$. This implies that admissible final attitudes with zero angular rate are never singular, for the attitude parameterization chosen.

Letting $s\Theta_f = 1$ and $c\Theta_f = 0$ in Eq. (7), the coordinate transformation matrix at the end of the pointing maneuver takes the form

$$\mathbb{T}_{AI}(\Psi_f, \Phi_f) = \begin{bmatrix} c\Phi_f c\Psi_f & c\Phi_f s\Psi_f & s\Phi_f \\ -s\Phi_f c\Psi_f & -s\Phi_f s\Psi_f & c\Phi_f \\ s\Psi_f & -c\Psi_f & 0 \end{bmatrix} \quad (11)$$

The second requirement (alignment of axis $\hat{\boldsymbol{\sigma}}$ with $\hat{\boldsymbol{r}}$) is enforced by equating the components of $\hat{\boldsymbol{\sigma}}$ and $\hat{\boldsymbol{r}} = \mathbb{T}_{AI} \hat{\boldsymbol{r}}_I$, when both vectors are expressed in \mathcal{F}_A , that is,

$$\begin{pmatrix} \cos \lambda \\ 0 \\ \sin \lambda \end{pmatrix} = \begin{pmatrix} \cos \Phi_f \cos \Psi_f \cos \alpha + \sin \Phi_f \sin \alpha \\ -\sin \Phi_f \cos \Psi_f \cos \alpha + \cos \Phi_f \sin \alpha \\ \sin \Psi_f \cos \alpha \end{pmatrix} \quad (12)$$

Equating the third components in Eq. (12), the precession angle Ψ_f must satisfy the condition

$$\sin \Psi_f = \sin \lambda / \cos \alpha \quad (13)$$

which admits two real solutions, $\Psi_{f,1} = \Psi_f^*$ and $\Psi_{f,2} = \pi - \Psi_f^*$, with $\Psi_f^* = \arcsin(\sin \lambda / \cos \alpha)$ if

$$|\alpha| \leq \pi/2 - |\lambda| \quad (14)$$

The inequality in Eq. (14) represents a feasibility condition for the pointing maneuver, that can be completed only when the elevation of the axis $\hat{\boldsymbol{r}}$ over the plane perpendicular to the angular momentum vector \boldsymbol{h} is less than the angular distance between $\hat{\boldsymbol{\sigma}}$ and $\hat{\boldsymbol{b}}$. Figure 2 shows the regions of admissible and forbidden target directions for a few values of λ .

The 1st and 2nd rows of Eq. (12) form a linear system of equations in the unknowns $X = \cos \Phi_f$ and $Y = \sin \Phi_f$, in the form

$$\begin{cases} aX + bY = c \\ bX - aY = 0 \end{cases} \quad (15)$$

where $a = \cos \Psi_f \cos \alpha$, $b = \sin \alpha$, and $c = \cos \lambda \geq 0$, whose solution is $X = ac/(a^2 + b^2)$, $Y = bc/(a^2 + b^2)$. Therefore, Φ_f

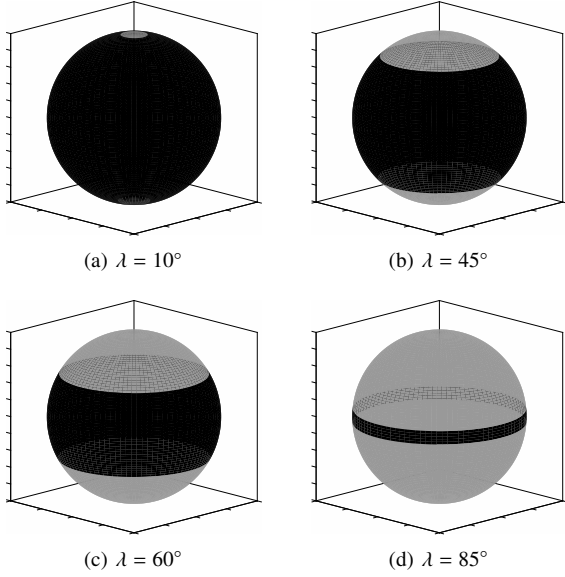


Figure 2. Admissible (black) and forbidden (grey) target directions in \mathcal{F}_I for different value of λ

can be found by using the four-quadrant inverse tangent function, that is, $\Phi_f = \text{atan2}(b, a) = \text{atan2}(\sin \alpha, \cos \alpha \cos \Psi_f)$. Two attitudes realize the single-axis pointing with spacecraft at rest, one for each solution of Eq. (13). Letting $\Phi^* = \text{atan2}(\sin \alpha, \cos \alpha \cos \Psi^*)$ and recalling the relation between Euler angles for \mathcal{F}_B and \mathcal{F}_A frames, one has

$$(\Psi, \Theta, \Phi)_f = \left\{ (\Psi^*, \pi/2, \Phi^* - \eta), (\pi - \Psi^*, \pi/2, \pi - \Phi^* - \eta) \right\} \quad (16)$$

2.4. Remarks

The constraint imposed by the conservation of the total angular momentum of the system made of the spacecraft platform and the two active reaction wheels provides some physical insight, useful for the derivation of a suitable control law. First of all, consider the total angular momentum vector expressed in body-frame components

$$\begin{pmatrix} J_1 \omega_1 + h_1 \\ J_2 \omega_2 + h_2 \\ J_3 \omega_3 \end{pmatrix} = H \begin{pmatrix} s\Phi s\Theta \\ c\Phi s\Theta \\ c\Theta \end{pmatrix} \quad (17)$$

The relationship between nutation angle Θ and angular velocity component along the failed axis $\hat{b} = \hat{e}_3$ is apparent. In particular, one has $\omega_3 = H/J_3 \cos \Theta$, which clearly implies that imposing a terminal value of $\omega_3 = 0$ is equivalent to require that $\Theta_f = \pi/2$. Thus, the two active reaction wheels can absorb the whole angular momentum vector, only if $\Theta = \pi/2$. This is equivalent to reducing the number of available rotational degrees of freedom to two.

It is also worthwhile to mention that, when the spacecraft is at rest, Eq. (17) implies that $h_1 = H_0 \sin \Phi_f$, $h_2 = H_0 \cos \Phi_f$. The angle Φ_f thus defines the allocation of the total angular momentum between the two active reaction wheels, which coincides with the desired final value of the spin angle for the auxiliary frame, \mathcal{F}_A .

3. Controller A: a Two-Stage Command Law

A two-stage control law is developed in this Section, where, as a first step, relative and total angular momentum are driven

towards the desired values at equilibrium, whereas accurate pointing is achieved as a second step for the pointing maneuver. More in detail, during the first phase the angular velocity ω is controlled and decreased towards zero, while the angular momentum is loaded into the two active reaction wheels. As outlined at the end of the previous section, the spacecraft is at rest when the angular momentum is distributed between the two active wheels, with $\mathbf{h}_f = H_0(\sin \Phi_f, \cos \Phi_f, 0)$. This causes spin and nutation angles to be driven towards their desired final values. Once ω and \mathbf{h} are sufficiently close to their target values, the controller switches to a different control mode, and the second step of the maneuver is performed, under the action of a Linear Quadratic Regulator (LQR).

In subsection 3.1., local properties of spacecraft dynamics under the action of an LQR controller are considered in the neighborhood of the desired final condition. An LQR controller is derived, which stabilizes Ψ , ω and \mathbf{h} to their specified values. The control law for the first step is developed in subsection 3.2., whereas the use of the LQR controller for arbitrarily large errors on precession angle Ψ is considered in subsection 3.3., where the control law for the second step is discussed.

3.1. Linearized System Analysis and Controller Design

In this section, the analysis of spacecraft rotational dynamics in the neighborhood of the desired target attitude is performed via a linearization of the complete set of nonlinear spacecraft equations of motion, namely Eqs. (8), (4), and (5).

The state vector, written in error form, is given by

$$\mathbf{x}^T = (e_\Psi, e_\Theta, e_\Phi, \omega^T, \mathbf{e}_h^T)$$

where $e_\Psi = \Psi - \Psi_f$, $e_\Theta = \Theta - \pi/2$, $e_\Phi = \Phi - \Phi_f$, and $\mathbf{e}_h = (h_1 - h_{1,f}, h_2 - h_{2,f})^T$. When higher-order terms are dropped, a linear time-invariant system of 8 first-order ordinary differential equations is obtained. Conservation of angular momentum allows one to drop three variables. A reduced-order linear system is thus derived, and one has

$$\begin{pmatrix} \dot{e}_\Psi \\ \dot{\omega} \\ \dot{e}_{h1} \end{pmatrix} = \begin{bmatrix} 0 & \mathbf{h}_f^T/H_0 & 0 \\ \mathbf{0} & -\mathbf{J}^{-1} \mathbf{h}_f^\times & \mathbf{0} \\ 0 & \mathbf{0}^T & 0 \end{bmatrix} \begin{pmatrix} e_\Psi \\ \omega \\ e_{h1} \end{pmatrix} + \begin{bmatrix} 0 \\ \mathbf{J}^{-1} \mathbf{S} \\ \mathbf{G} \end{bmatrix} \mathbf{u} \quad (18)$$

where $\mathbf{x} = (e_\Psi, \omega^T, e_{h1})^T$ is the state vector, \mathbf{u} is the control vector, $\mathbf{0} = (0, 0, 0)^T$, $\mathbf{G} = (-1, 0)$, and

$$\mathbf{S} = \begin{bmatrix} 1 & 0 & 0 \\ 0 & 1 & 0 \end{bmatrix}$$

This choice of the state vector elements guarantees that, when the reduced-order system reaches the origin, the remaining variables also approach their desired values. In fact, $\Theta \rightarrow \pi/2$ for $\omega_3 \rightarrow 0$, while $\omega \rightarrow 0$ and $h_1 \rightarrow h_{f1}$ imply $h_2 \rightarrow h_{f2}$, which leads to $\Phi \rightarrow \Phi_f$.

The system in Eq. (18) is controllable if the controllability matrix $C = [B, AB, A^2B, A^3B, A^4B]$ has full rank. Letting $K_s = (J_2 h_{f2}^2 + J_1 h_{f1}^2) / (J_1 J_2 J_3)$ and $K_d = (J_1 - J_2) / (H_0 J_1 J_2 J_3)$, it is

$$C = \begin{bmatrix} 0 & 0 & \frac{h_{f1}}{H_0 J_1} & \frac{h_{f2}}{H_0 J_2} & 0 & 0 & K_d \frac{h_{f1} h_{f2}^2}{J_1} & -K_d \frac{h_{f1}^2 h_{f2}}{J_2} & 0 & 0 \\ \frac{1}{J_1} & 0 & 0 & 0 & -\frac{h_{f2}^2}{J_1^2 J_3} & \frac{h_{f1} h_{f2}}{J_1 J_2 J_3} & 0 & 0 & K_s \frac{h_{f2}^2}{J_1^2 J_3} & K_s \frac{h_{f2} h_{f1}}{J_1 J_2 J_3} \\ 0 & \frac{1}{J_2} & 0 & 0 & \frac{h_{f1} h_{f2}}{J_1 J_2 J_3} & -\frac{h_{f1}^2}{J_2^2 J_3} & 0 & 0 & -K_s \frac{h_{f2} h_{f1}}{J_1 J_2 J_3} & -K_s \frac{h_{f1}^2}{J_2^2 J_3} \\ 0 & 0 & -\frac{h_{f2}}{J_1 J_3} & \frac{h_{f1}}{J_2 J_3} & 0 & 0 & K_s \frac{h_{f2}}{J_1 J_3} & -K_s \frac{h_{f1}}{J_2 J_3} & 0 & 0 \\ -1 & 0 & 0 & 0 & 0 & 0 & 0 & 0 & 0 & 0 \end{bmatrix} \quad (19)$$

Sufficient condition for controllability is that all 5 rows of C are linearly independent. By inspecting the expression of C , one can note that all pairs of rows are linearly independent, with two relevant exceptions, that is, i) rank of C drops to 2 if $h_{f1} = h_{f2} = 0$, but this condition is ruled out by the fact that $\|\mathbf{h}\|_f = H_0 > 0$, and ii) rows 2 and 5 are no longer linearly independent if $h_{f2} = 0$, that is, for $\Phi_f = \pm\pi/2$. The latter is a consequence of the selection of e_{h1} in the state vector of the reduced order model, in place of h_2 . If one considers the dual reduced-linear system obtained by selecting h_2 instead of h_1 as the 5-th state variable, a controllable linear time-invariant system is obtained for $h_{f1} \neq 0$. As a result, the nonlinear system is first-order controllable, provided that an appropriate choice of state variable is performed, in order to account for the peculiar case of $\Phi_f = \pm\pi/2$. In what follows it will be assumed that $\Phi_f \neq \pm\pi/2$.

A static full-state feedback control law in the form $\mathbf{u} = \mathbf{K}\mathbf{x}$, which stabilizes the linearized system of Eq. (18) about the origin, is synthesized in the framework of LQR control theory.¹²⁾ This method provides a robust and rigorous approach to determine the optimal control gain matrix $\mathbf{K} \in \mathbb{R}^{2 \times 5}$ that minimizes a quadratic merit index defined as

$$\mathcal{J} = \int_0^\infty (\mathbf{x}^T \mathbf{Q} \mathbf{x} + \mathbf{u}^T \mathbf{R} \mathbf{u}) dt$$

where $\mathbf{Q} \in \mathbb{R}^{5 \times 5}$ and $\mathbf{R} \in \mathbb{R}^{2 \times 2}$ are positive definite weighting matrices for state perturbation and control action, respectively. The solution of the Algebraic Riccati Equation

$$\mathbf{A}^T \mathbf{P} + \mathbf{P} \mathbf{A} - \mathbf{P} \mathbf{B} \mathbf{R}^{-1} \mathbf{B}^T \mathbf{P} + \mathbf{Q} = 0$$

provides the optimal value of the gain control matrix, given by $\mathbf{K} = \mathbf{R}^{-1} \mathbf{B}^T \mathbf{P}$.

The LQR controller guaranties asymptotic stability and optimal closed-loop performance only locally, in a neighborhood of some equilibrium point. Nonetheless, in the present case, the state matrix \mathbf{A} does not explicitly depend on the value of Ψ_f . As a result, for a given spacecraft and a particular choice of the weighting matrices, \mathbf{Q} and \mathbf{R} , the optimal gain control matrix \mathbf{K} does not depend on Ψ_f , as well.

3.2. Step I: Angular Momentum Stabilization

For the present application, the LQR controller is developed in the neighborhood of the equilibrium point $e_\Psi = 0$, $\omega = 0$, $\mathbf{h} = \mathbf{h}_f$, such that also $\Theta = \pi/2$ and $e_\Phi = 0$. However, in a practical generic case, one cannot expect that the initial state is close to the desired equilibrium. In order to achieve global convergence capabilities for the closed-loop system, a controller based on the complete nonlinear equations of motion is to be designed, which drives the spacecraft sufficiently close to the prescribed alignment, with a small residual angular rate.

Consider the strictly positive candidate Lyapunov function,

$$V = \frac{1}{2} \omega^T \mathbf{J} \omega + K_h (\mathbf{e}_h)^T \mathbf{e}_h \quad (20)$$

where $\mathbf{e}_h = \mathbf{h} - \mathbf{h}_f$, with $\mathbf{h}_f = (H_0 \sin \Phi_f, H_0 \sin \Phi_f, 0)^T$. Note that, as a difference with respect to the linear controller defined in the previous subsection, the error vector for the relative angular momentum now features three components.

By taking the time derivative of Eq. (20) one gets

$$\dot{V} = \omega^T \mathbf{u} - K_h \mathbf{e}_h^T \mathbf{u} = (\omega - K_h \mathbf{e}_h)^T \mathbf{u} \quad (21)$$

that can be made negative semi-definite by choosing

$$\mathbf{u} = \mathbf{K}_p (\omega - K_h \mathbf{e}_h) \quad (22)$$

with \mathbf{K}_p an arbitrary positive definite gain matrix. A simple form, such as $\mathbf{K}_p = K_p \mathbb{I}_3$, suits the needs of the controller, where \mathbb{I}_3 is the identity matrix of order three, and the value of K_p can be selected by trial-and-error, evaluating in simulation the closed-loop performance of the controller.

Note that \dot{V} does not depend on ω_3 , as u_3 remains identically zero during the maneuver, and consequently \dot{V} is only negative semi-definite. Nevertheless, La Salle invariance principle can be invoked to assess system stability. In fact, the system must converge towards a solution $\mathbf{x}(t)$ such that $\dot{V} = 0$, which implies $(\omega_1, \omega_2, \omega_3, h_1, h_2) = (0, 0, \Omega, 0, 0)$. However, when the error on the relative angular momentum is zero ($\mathbf{e}_h = 0$), it is also $\|\mathbf{h}_f\| = H_0$. Because of conservation of total angular momentum, a value of $\Omega = 0$ is the only admissible solution. Thus, the control law in Eq. (22) globally asymptotically stabilizes the system towards the condition $\omega = 0$, $\mathbf{e}_h = 0$.

3.3. Step II: Linear Controller

When the non-linear controller described in the above subsection, Eq. (22), achieves a condition such that $\|\omega\| < \varepsilon_\omega$ and $e_\Phi < \varepsilon_\Phi$, the LQR control law is activated. The activation thresholds ε_ω and ε_Φ were selected by a trial-and-error procedure, that demonstrated that ε_Φ has a limited impact on closed-loop performance, whereas ε_ω needs to be small, but not too close to zero. For the present application, the following values were used: $\varepsilon_\omega = 0.01$ rad/s and $\varepsilon_\Phi = 1$ deg. As a matter of fact, the possibility of varying the angle Ψ is related to the value of the residual angular velocity. This explains the reason for the threshold on $\|\omega\|$ should not be too close to zero.

Note that at the end of Step I, the errors on angular rate, relative angular momentum, spin and nutation angles are all expected to be small, whereas the error on Ψ can be large, apparently hindering the validity of the optimal closed-loop performance of the LQR controller, which are valid only locally, closed to the considered equilibrium. Nonetheless, when all the other quantities are close to their equilibrium values, the evolution of Ψ achieves a linear formulation for arbitrary values

of Ψ , thus preserving the validity of the optimality of the LQR controller.

4. Controller B: A Fully Nonlinear Control Law

The derivation of a single-step control law aiming at stabilizing the spacecraft about the target attitude (Ψ_f, Φ_f) is now presented. The set of nonlinear equations of motion, given by Eq.s (8), (4), (5), matches the standard form of cascade systems, where precession angle dynamics

$$\dot{\Psi} = \frac{1}{\sin \Theta} (\sin \Phi, \cos \Phi, 0)^T \omega \quad (23)$$

is driven by the other system variables, whereas the remaining part of the system does not depend on Ψ .

By imposing the tracking of the following angular velocity

$$\omega_{des} = -K_\Psi (\sin \Phi \cos \Phi, 0)^T e_\Psi \quad (24)$$

the asymptotically stable dynamics for $e_\Psi = \Psi - \Psi_f$ is obtained. The proof is straightforward: let V_1 be a positive Lyapunov candidate

$$V_1 = \frac{1}{2} e_\Psi^2 \quad (25)$$

Under the assumption of exact tracking (i.e. $\omega = \omega_{des}$) and $\sin \Theta \neq 0$, the time derivative of V_1 is

$$\dot{V}_1 = -\frac{K_\Psi}{\sin \Theta} e_\Psi^2 \quad (26)$$

which is negative definite for any $K_\Psi > 0$.

On the basis of this last result, a control law is designed to track simultaneously ω_{des} and \mathbf{h}_f . After defining the tracking error for the angular velocity components as $\mathbf{e}_\omega = \omega - \omega_{des}$, the system can be recast in the form

$$\dot{e}_\Psi = -K_\Psi e_\Psi + \frac{1}{\sin \Theta} [\sin \Phi, \cos \Phi, 0] e_\omega \quad (27)$$

$$\dot{\mathbf{e}}_\omega = -\mathbf{e}_\omega \times (\mathbf{J}\omega + \mathbf{h}) + \mathbf{u} - \omega_d \times \mathbf{H} - \dot{\omega}_d \quad (28)$$

$$\dot{\mathbf{e}}_h = -\mathbf{u} \quad (29)$$

matching the perturbed system structure, $\dot{\mathbf{x}} = \mathbf{f}(\mathbf{x}, \mathbf{u}) + \mathbf{g}(\mathbf{x})$, where

$$\dot{\mathbf{x}} = \begin{pmatrix} \dot{e}_\Psi \\ \dot{\mathbf{e}}_\omega \\ \dot{\mathbf{e}}_h \end{pmatrix}; \quad \mathbf{f}(\mathbf{x}) = \begin{pmatrix} -(K_\Psi / \sin \Theta) e_\Psi \\ -\mathbf{e}_\omega \times (\mathbf{J}\omega + \mathbf{h}) + \mathbf{u} \\ -\mathbf{u} \end{pmatrix} \quad (30)$$

represents the nominal system, and

$$\mathbf{g}(\mathbf{x}) = \begin{cases} (1/\sin \Theta) [\sin \Phi, \cos \Phi, 0] e_\omega \\ -\omega_d \times \mathbf{H} - \dot{\omega}_d \\ \mathbf{0} \end{cases} \quad (31)$$

is a vanishing perturbation term, with $\dot{\omega}_{des}$ and $\omega_{des} \rightarrow 0$ as $e_\Psi \rightarrow 0$. Inspection of Eq. (31) allows one to state that $\mathbf{g}(\mathbf{x}) < \gamma \|\mathbf{x}\|$, at least in a region near the equilibrium, where $\Theta \in (0, \pi)$. Let V_e a positive definite Lyapunov candidate

$$V_e = \frac{1}{2} e_\Psi^2 + \frac{1}{2} \mathbf{e}_\omega^T \mathbf{J} \mathbf{e}_\omega + \frac{1}{2} K_h \mathbf{e}_h^T \mathbf{e}_h \quad (32)$$

whose time derivative is

$$\dot{V}_e = -K_\Psi e_\Psi^2 + (\mathbf{e}_\omega - K_h \mathbf{e}_h)^T \mathbf{u}$$

By choosing

$$\mathbf{u} = -K_p (\mathbf{e}_\omega - K_h \mathbf{e}_h) \quad (33)$$

one has

$$\dot{V}_e = -K_\Psi e_\Psi^2 - (\mathbf{e}_\omega - K_h \mathbf{e}_h)^T \mathbf{u}$$

Since \dot{V}_e does not depend on ω_3 , \dot{V} is negative semi-definite and La Salle invariance principle is invoked to assess system stability. As a matter of fact, the system must converge towards a solution $\mathbf{x}(t)$ such that $\dot{V} = 0$, which implies $(e_\Psi, e_{\omega 1}, e_{\omega 2}, e_{\omega 3}, e_{h1}, e_{h2}) = (0, 0, 0, \tilde{e}_\Omega, 0, 0)$. Conservation of total angular momentum can be invoked here to prove that $e_\Omega = 0$ is the only admissible solution when the error on the relative angular momentum is zero ($\mathbf{e}_h = 0$). Thus, the control law in Eq. (33) provides global asymptotical stability to the unperturbed system about the origin. Nonetheless, asymptotic stability of the origin of the nominal system does guarantee the robustness of the stability of the equilibrium to the vanishing perturbation $\mathbf{g}(\mathbf{x})$ in a global sense. This latter aspect is the subject of ongoing analysis and will be here investigated by numerical simulation only.

5. Results

A spacecraft with an inertia tensor $\mathbf{J} = \text{diag}(10, 8, 9)$ kg m² is considered for demonstrating the viability of the proposed control methodologies and analyzing and comparing the resulting closed-loop performance for Controllers A and B. The two active reaction wheels have an identical moment of inertia, $J_w = 0.0077$ kg m². Wheel electric motor torque saturation is set at 20 mNm. Spacecraft data are representative of a small satellite. The control approach was also tested for different sets of spacecraft parameters, in order to assess the results for a wide variety of system configurations. These latter results are not reported here, for the sake of conciseness, as far as the behavior of the system appears qualitatively similar to the cases presented in what follows.

5.1. Convergence for Controller B

Before comparing Controllers A and B, results of a Monte Carlo simulation are reported, in order to assess convergence characteristics of the closed-loop system featuring Controller B, that is not proven to be globally stable. A set of 1000 runs is performed, randomly selecting the initial attitude, for a prescribed value of initial angular momentum $H_0 = 0.85$ N m s. The positions of target direction and body-fixed axis are selected such that the maneuver is feasible, with $\lambda = 5$ deg and $\alpha = 45$ deg. Control law gains are equal to $K_p = 0.25$, $K_\Psi = 0.1$, and $K_h = 0.1$.

Figure 3 shows the pointing error of axis $\hat{\sigma}$ with respect to the desired direction $\hat{\tau}$ as a function of time. The error is plotted on a logarithmic scale, and it appears that an exponential convergence is obtained for all the considered initial conditions. Convergence time to various degree of pointing precision is reported in Table 1, in terms of average value for reaching a pointing error below 1, 0.1 and 0.01 deg, respectively. The standard deviation of convergence time for the considered population of solutions is also reported. Its value is apparently unaffected by the required level of pointing precision.

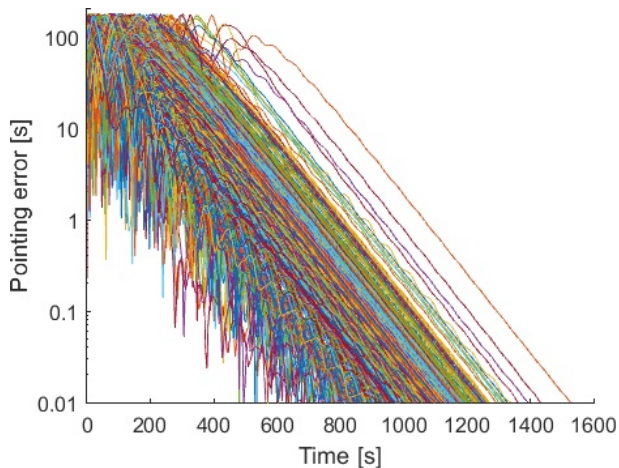


Figure3. Monte Carlo analysis for Controller B.

Table1. Convergence time for Controller B in the Monte Carlo analysis.

	$e = 1^\circ$	$e = 0.1^\circ$	$e = 0.01^\circ$
mean	603	831	1060
std	98	100	101

The statistical properties of convergence time depend on the values of the control gains. The values reported above and used for the Monte Carlo analysis were selected by a simple trial-and-error procedure performed on a limited number of test cases, without an actual optimization with respect to average performance (aiming at a fast convergence) and repeatability of the results (requiring a small value of the standard deviation). Nonetheless, the choice appears reasonable.

5.2. Comparison between Controllers A and B

A comparison between closed-loop performance for Controllers A and B is now possible. In this section, unless otherwise stated in the figure label, a blue line indicates the time histories of relevant variables for Controller A. A solid line is used for stage 1 (nonlinear controller driving ω to zero) and a dashed one for stage 2 (final convergence under the action of the LQR controller). A solid red line indicates the variation with time of the same variables under the action of Controller B.

Figures 4 and 5 report the variations of pointing error and magnitude of the angular velocity as a function of time, respectively, for Controllers A and B, starting from the same initial condition. An oscillatory convergence is obtained for Controller B, in terms of pointing error, whereas the pointing error reaches a steady (and indeed large) value under the action of the nonlinear control law for stage 1 of controller A. In the same time interval, the angular speed is brought close to zero by both controllers (see Fig. 5 for $t \approx 300$ s), with the spin angle reaching its desired value for both controllers (blue and red lines in Fig. 6).

Conversely, the error on the precession angle is monotonically reduced by Controller B (red line in Fig. 7), whereas, it reaches a finite (and once again large) value, during step 1, when using Controller A. As expected, in this latter case, the pointing error at the end of step 1 is mainly due to an error on the (uncontrolled) precession angle. When the LQR controller takes over, an initial acceleration transient is present, where the angular rate is incremented by the control logic, in order to

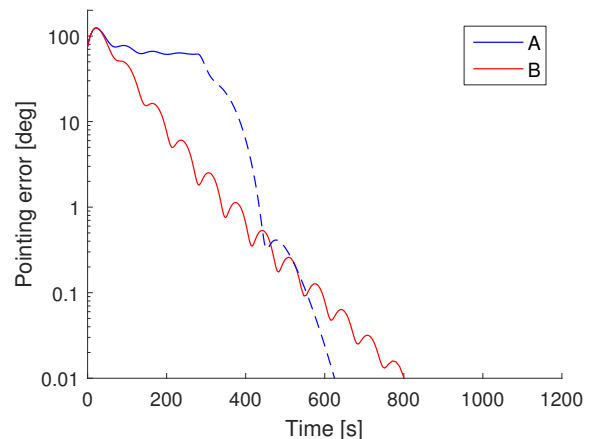


Figure4. Comparison between Controllers A and B: pointing error

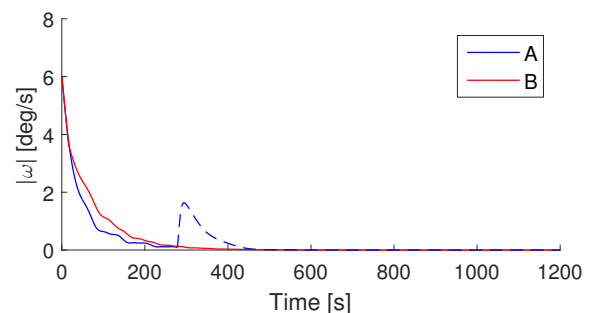


Figure5. Comparison between Controllers A and B: angular velocity magnitude

achieve a precession rate for driving also Ψ towards its desired value (dashed blue line in Fig. 7).

In this latter respect, a “bump” in the value of angular rate magnitude is clearly visible for $300 < t < 450$ s (see the initial portion of the dashed blue line in Fig. 5), which is obtained by a control action on the wheels, as it is apparent from the upper plot in Fig. 8. In this respect, the control action for Controller B

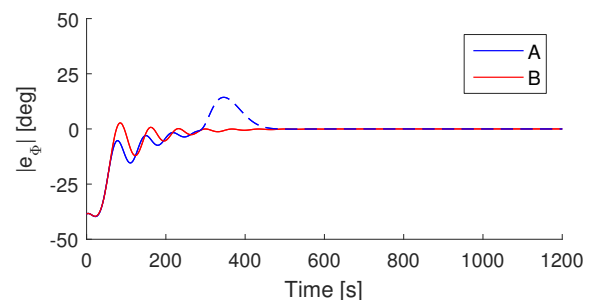


Figure6. Comparison between Controllers A and B: error on spin angle

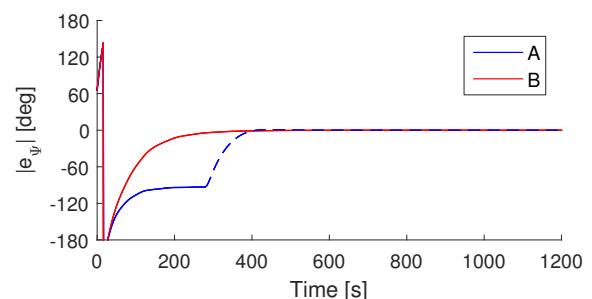


Figure7. Comparison between Controllers A and B: error on precession angle

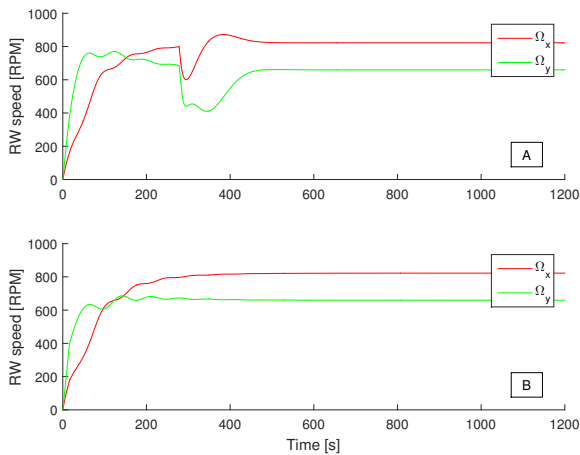


Figure 8. Comparison between Controllers A and B: wheel rates

(bottom plot in the same figure) appears smoother. Obviously, both control laws drive the active wheels to the same final spin condition.

5.3. Comments

If on one side, the use of the two-step control architecture appears attractive, given the rigorous proof of global stability, on the other hand the switching logic needs to be carefully analyzed in practice. The proof of convergence is obtained without taking into account wheel rate or torque saturation. After the switching, and in the presence of large errors on Ψ , the need for accelerating the spacecraft towards its final desired attitude may lead to wheel saturation and, possibly, divergence, when this issue is not adequately addressed.

This phenomenon can be avoided by a careful choice of the weighting gain matrices in the LQR controller synthesis, where the weight for angular rate components is increased, in order to penalize large angular rates, and the weight for precession angle errors is simultaneously reduced. In the present application, the weight matrices $\mathbf{Q} = \text{diag}(0.1, 100, 100, 100, 1)$ and $\mathbf{R} = \text{diag}(100, 100)$ provided an LQR controller robust to the switching phase and the following acceleration transient, for the considered level of wheel motor torque saturation. Also, the switching threshold on angular rate needs to be carefully selected, as the “bump” phenomenon is increased when step 1 ends with a very small final angular rate.

All in all, the closed loop behaviour of Controller B appears in general smoother, with monotonic or almost monotonic convergence for most variables and a smooth wheel rate profile. The pointing convergence rate of Controller B is faster, for large errors, but it becomes slower for small values of the pointing error, where the optimal characteristics of the LQR controller provide an advantage in terms of convergence speed locally, in the neighborhood of the desired attitude.

6. Conclusion

In this paper two control laws were derived, which allow for aiming an arbitrary body-fixed axis along a prescribed inertial direction, in the presence of a non-zero angular momentum for the spacecraft. A feasibility condition for the desired pointing maneuver was provided, together with the final attitude that achieves the desired pointing with zero residual angular rate.

A two-step control law was discussed first, where the first step drives the angular rate to zero, while taking spin and nutation angles to their desired values. A second step, under the action of a Linear Quadratic Regulator was added for completing convergence to the final attitude. A second nonlinear controller was then considered, where global convergence from arbitrary initial conditions is proven by means of numerical simulation only, by means of a Monte Carlo analysis.

An extensive set of simulation was performed for comparing closed-loop performance of the two controllers. The two-step control law has a guaranteed performance capability, from arbitrary initial conditions. Nonetheless, the nonlinear controller, provides a smoother control action and an almost monotonic convergence to the final desired state.

References

- 1) Tsiotras, P. and Doumchenko, V., “Control Of Spacecraft Subject To Actuator Failures: State-Of-The-Art And Open Problems,” *Problems, Proceedings of the R.H. Battin Astrodynamics Symposium, College Station, TX, March 20-21, 2000, AAS Paper*, pp. 00–264.
- 2) Tsiotras, P. and Longuski, J. M., “Spin-axis stabilization of symmetric spacecraft with two control torques,” *Systems & Control Letters*, Vol. 23, No. 6, 1994, pp. 395–402.
- 3) Kim, S. and Kim, Y., “Spin-Axis Stabilization of a Rigid Spacecraft Using Two Reaction Wheels,” *Journal of Guidance, Control, and Dynamics*, Vol. 24, No. 5, Sept. 2001, pp. 1046–1049.
- 4) Yamada, K., Takatsuka, N., and Shima, T., “Spacecraft pointing control using a variable-speed control moment gyro,” *Transactions of the Japan Society for Aeronautical and Space Science, Space Technology Japan*, Vol. 7, No. ists26, 2009, pp. Pd_1–Pd_6.
- 5) Tsiotras, P., Corless, M., and Longuski, M., “A Novel Approach to the Attitude Control of Axisymmetric Spacecraft,” *Automatica*, Vol. 31, No. 8, 1995, pp. 1099–1112.
- 6) Horri, N. M. and Palmer, P., “Practical Implementation of Attitude-Control Algorithms for an Underactuated Satellite,” *Journal of Guidance, Control, and Dynamics*, Vol. 35, No. 1, Jan. 2012, pp. 40–45.
- 7) Zavoli, A., De Matteis, G., Giulietti, F., and Avanzini, G., “Single-Axis Pointing of an Underactuated Spacecraft Equipped with Two Reaction Wheels,” *Journal of Guidance, Control, and Dynamics*, March 2017, pp. 1–7.
- 8) Yoon, H. and Tsiotras, P., “Spacecraft line-of-sight control using a single variable-speed control moment gyro,” *AIAA Journal of Guidance, Control, and Dynamics*, Vol. 29, No. 6, 2006, pp. 1295.
- 9) Kwon, S., Shimomura, T., and Okubo, H., “Pointing control of spacecraft using two SGCMGs via LPV control theory,” *Acta Astronautica*, Vol. 68, No. 7, 2011, pp. 1168–1175.
- 10) Hughes, P. C., *Spacecraft attitude dynamics*, Dover Publications, Mineola, N.Y., 2004.
- 11) Wie, B., *Space vehicle dynamics and control*, Aiaa, 1998.
- 12) Haddad, W. M. and Chellaboina, V., *Nonlinear dynamical systems and control: a Lyapunov-based approach*, Princeton University Press, 2008.